# Soluble and cell-bound forms of steel factor activity play distinct roles in melanocyte precursor dispersal and survival on the lateral neural crest migration pathway

Wehrle-Haller, Bernhard; Weston, J A

Development 121, 731-742 (1995)
Printed in Great Britain © The Company of Biologists Limited 1995



# Soluble and cell-bound forms of steel factor activity play distinct roles in melanocyte precursor dispersal and survival on the lateral neural crest migration pathway

**Bernhard Wehrle-Haller and James A. Weston**

Institute of Neuroscience, University of Oregon, Eugene, OR 97403, USA

Email: Weston@UONEURO.UOREGON.EDU

## SUMMARY

**Trunk neural crest cells segregate from the neuroepithelium and enter a 'migration staging area' lateral to the embryonic neural tube. After some crest cells in the migration staging area have begun to migrate on a medial pathway, a subpopulation of crest-derived cells remaining in the migration staging area expresses mRNAs for the receptor tyrosine kinase, c-kit, and tyrosinase-related protein-2, both of which are characteristic of melanocyte precursors. These putative melanocyte precursors are subsequently observed on the lateral crest migration pathway between the dermatome and overlying epithelium, and then dispersed in nascent dermal mesenchyme.**

**Melanocyte precursors transiently require the c-kit ligand, Steel factor for survival. Although Steel factor mRNA is transiently expressed in the dorsal dermatome before the onset of trunk neural crest cell dispersal on the lateral pathway, it is no longer produced by dermatomal cells when melanocyte precursors have dispersed in the dermal mesenchyme. To assess the role of Steel factor in migration of melanocyte precursors on the lateral pathway, we analyzed melanocyte precursor dispersal and fate on the lateral pathway of two different *Sl* mutants, *Sl*, a null allele, and $Sl^d$, which lacks cell surface-associated Steel factor but produces a soluble form. No melanocyte precursors were detected in the dermatome of embryos homozygous for the *Sl* allele or in *W* mutants that lack functional c-kit. In contrast, in embryos homozygous for the $Sl^d$ allele, melanocyte precursors appeared on the lateral pathway, but subsequently disappear from the dermis. These results suggest that soluble Steel factor is required for melanocyte precursor dispersal on the lateral pathway, or for their initial survival in the migration staging area. In contrast, membrane-bound Steel factor appears to promote melanocyte precursor survival in the dermis.**

Key words: Steel factor, melanocyte precursor, neural crest, c-kit, TRP-2

## INTRODUCTION

In the trunk of vertebrate embryos, neural crest cells segregate from the neural epithelium and transiently reside in a 'migrating staging area' (MSA) delimited by the neural tube, the somite and the overlying epithelium. Crest cells immediately begin to disperse from the MSA on a ventromedial pathway along the myotome and into rostral sclerotomal mesenchyme (Erickson and Loring, 1987; Weston, 1991). Later, crest cells remaining in the MSA disperse on a dorsolateral pathway, migrating between the dermatome and the epidermis (Erickson et al., 1992). The crest cells on the lateral pathway subsequently become interspersed with dermal mesenchyme and cross the epithelial basement membrane to localize in the epidermis. In the mouse, these cells remain in the epithelium for many days before they undergo melanogenesis postnatally. Before early markers for pigment cell precursors were available, the timing of melanocyte precursor dispersal and localization in the skin was inferred by testing for the ability of cultured or grafted tissue to produce melanocytes (Rawles 1947; Derby 1978). Results of such studies revealed that the first melanocyte precursors are present on the lateral pathway of the embryonic trunk at about e11 and reach the limb buds by e12. At a lateral trunk level most of the melanocyte precursors enter the epidermis between e13 and e14 (Mayer, 1973). Recently, histochemical reagents that intensify pigment in melanosomes of otherwise undifferentiated melanocytes, or probes for melanocyte markers such as the tyrosine kinase receptor, c-kit, and tyrosinase-related protein-2 (TRP-2) confirmed these inferences, and revealed the presence of melanocyte precursors in the head as early as e10.5 (Manova and Bachvarova, 1991; Steel et al., 1992; Pavan and Tilghman, 1994).

Several mouse mutations affecting coat pigmentation have been described and their molecular defects characterized. Two of the best studied, *Steel* (*Sl*) and *Dominant spotting* (*W*), are embryonic lethals as homozygotes, due to failure of erythropoiesis, whereas heterozygous embryos are viable but eventually show a white spotting coat color pattern. The defective gene in *W* mutants codes for a receptor tyrosine kinase (c-kit;

Geissler et al., 1988) and its growth factor ligand, variously called Steel Factor (SlF), Stem cell factor (SCF), mast cell growth factor (MCF) or kit ligand (KL) (Anderson et al., 1990; Copeland et al., 1990; Huang et al., 1990; Nocka et al., 1990a; Williams et al., 1990; Flanagan and Leder, 1990) is encoded at the *Sl* locus. For both genes, less severe alleles have been described that are viable as homozygotes, but show a white coat, anaemia and sterility (see Morrison-Graham and Takahashi, 1993; Copeland et al., 1990; Flanagan et al., 1991; Brannan et al., 1991; Duttlinger et al., 1993).

A number of in vivo and in vitro approaches have been initiated to pinpoint the critical period when SlF or c-kit activity is required for survival of pigment precursors. For example, an early function for c-kit and SlF is suggested by expression of c-kit mRNA in cells found dorsal and lateral to the somites (Manova and Bachvarova, 1991) and the presence of SlF mRNA in the somitic dermatome at around e10.5 (Matsui et al., 1990). In utero injection of c-kit blocking antibody has revealed an early (e10.5), an intermediate (e14.5) and a late effect of c-kit function on melanogenesis (Nishikawa et al., 1991; Yoshida et al., 1993). Consistent with these inferences, analysis of melanogenesis in vitro has shown that SlF is transiently required for melanogenic precursor survival between day 2 and 6.5 in culture (equivalent to e11.5-16; Morrison-Graham and Weston, 1993).

SlF is normally expressed in two splice-variants, both of which are initially localized to the cell surface. The larger variant contains an extracellular proteolytic cleavage site, which permits release of SlF from the cell surface. The smaller splice-variant is usually not cleaved and normally remains associated with the cell surface (Flanagan et al., 1991; Huang et al., 1992; see also Williams et al., 1992). Although fragmentary distribution and mutational analysis of the influence of the c-kit/SlF system on melanocyte precursors exists (Steel et al., 1992), it is not yet clear whether the functions of alternatively spliced SlF are different, or even what such functions might be.

An opportunity to address this issue is provided by assessing the early morphogenetic behavior and fate of melanocyte precursors in embryos carrying various mutations at the *Steel* locus. For example, in the *Steel-dickie* ($Sl^d$) allele, the transmembrane and cytoplasmic domains of SlF are deleted so that only a secreted form of SlF is produced (Flanagan et al., 1991; Brannan et al., 1991). In spite of the presence of SlF activity (Brannan et al., 1991), mice heterozygous for $Sl^d$ exhibit a distinct coat color phenotype. Embryos homozygous for this allele are viable but exhibit characteristic phenotypes including lack of coat pigmentation. In these mutants, melanocyte precursors are initially present in the head but fail to survive (Steel et al., 1992). It is not yet known, however, how these phenotypes arise, or if the migration behavior and growth factor requirements of trunk and head melanocyte precursors are different.

In the present study, we have examined the early dispersal and fate of melanocyte precursors in *Sl* (null) and $Sl^d$ mutants to elucidate the function of SlF in determining the early pigment patterns, and to distinguish the role(s) of the soluble and cell-bound forms of SlF in regulating the early migration behavior of pigment cell precursors. Thus, we have characterized melanocyte precursor appearance in the MSA, and their dispersal and fate in relation to the time and location of SlF mRNA expression in normal embryos and embryos homozygous for two *Steel* alleles. Our results indicate that migrating melanocyte precursors respond to cues provided by diffusible (soluble) SlF, through activation of the c-kit receptor. We conclude that soluble SlF is sufficient for responsive melanoblast precursors to initiate their dispersal onto the lateral pathway in vivo, but that cell-bound SlF is necessary for subsequent survival of pigment cells in the newly formed dermal mesenchyme.

## MATERIALS AND METHODS

### Genotyping mouse embryos

Inbred colonies of B6, B6$Sl^d$, WBReSl and WBW were maintained in our laboratory. Dated matings were set up in the evening and plugs checked the following morning. The presence of a plug was considered as e0.5.

Since *Sl*, $Sl^d$ and *W* homozygous are sterile, we mated heterozygous mice to obtain homozygous embryos. *Sl*, $Sl^d$ or *W* homozygous embryos can only be recognized by morphological criteria after about e15.5, when their liver appears pale compared to wild-type or `heterozygous littermates. In order to identify the genotype of the *Sl* and $Sl^d$ embryos earlier, we amplified a genomic sequence present in the *Steel* gene, which is deleted in the *Sl* (Copeland et al., 1990) and $Sl^d$ (Flanagan et al., 1991) mutations. According to Steel et al. (1992) we used a set of primers from the 7th and 8th exon respectively to amplify a 700 bp fragment containing mainly intron sequences. Genomic DNA was isolated from excised limb buds by proteinase K and 0.5% SDS extraction and ethanol precipitation. Following an amplification with 35 cycles (45 seconds at 93°C, 1 minute at 56°C, 1 minute at 72°C) a 700 bp fragment was detected on a 1% agarose gel. Both *Sl/Sl* and $Sl^d/Sl^d$ embryos could be identified by the absence of that amplified band. As a control for the quality of the genomic DNA as well as the amplification reaction (PCR), we used an alternative set of primers, amplifying a 500 bp genomic fragment from the gene coding for PDGFRα located on chromosome 5 (Orr-Urtreger et al., 1992). We performed separate amplifications with the same template DNA or included both sets of primers in one reaction. The following primers were used: *Sl* forward primer CCATGGCATTGCCGGCTCTC (bases 665 to 684; Huang et al., 1990) and *Sl* reverse primer CTGCCCTTGTAAGACTTGACTG (complement of bases 757 to 736). PDGFRα forward primer ACCTCCTTTCGGACGATGAC (bases 2417 to 2436; Wang et al., 1990, Acc# M57683) located within the interkinase region and a reversed genomic primer corresponding to a sequence located within an intron 500 bp apart ATCACTTCAGAATGGCTCCA (Peter Lonai; personal communication).

Embryos homozygous for the *W* gene, could not be identified using a PCR approach since the *W* (null) allele is a point mutation in a splice site (Hayashi et al., 1991), which generates a nonfunctional c-kit protein (Nocka et al., 1990b). Therefore, all embryos from a litter produced by mating heterozygotes were treated identically, and their mutant phenotype assessed by the localization of melanocyte precursors (see below). As expected, a quarter of all the embryos scored by PCR were homozygous for either *Sl* or $Sl^d$, or were identified as *W* homozygotes by their pigment pattern.

### cDNA probes and antibodies

cDNAs for c-kit were kindly provided by Dr Robert J. Arceci (Boston), for Steel factor (KL-M1) by Dr John Flanagan (Boston) and TRP-2 by Dr Ian Jackson (London). Polyclonal anti-fibronectin and laminin were obtained from Collaborative Research. Rhodamine goat anti-rabbit was from Cappel.

Digoxigenin (DIG)-labeled sense and antisense riboprobes were

generated using a standard protocol (Boehringer Mannheim) from linearized plasmids and used for whole-mount in situ hybridization at concentrations of 1 μg/ml. RNA synthesis was checked by agarose gel electrophoresis.

### Whole-mount in situ hybridization and antibody staining

Whole-mount in situ hybridization was performed according to Yamaguchi et al. (1992; Y. Takahashi, personal comm.). The hybridization of DIG-labeled single-stranded RNA probes was detected with anti-DIG antibodies coupled to alkaline phosphatase. Details of the protocol will be provided upon request.

As a control for the specificity of our in situ protocol, we hybridized with sense riboprobes for KL-M1 and c-kit under identical conditions. We were not able to generate a sense probe from our plasmid containing the TRP-2 probe. No staining could be detected in embryos hybridized with any of the sense probes. In experimental and control embryos, occasionally unspecific stain could be detected in the lumen of the spinal cord, otic vesicle and brain vesicles. Puncture of the hindbrain did reduce this unspecific trapping of stain. Embryos from e9.5 to e13.5 were treated identically with the exception of prolonging the proteinase K treatment for older embryos to enhance penetration of the probes. It must be emphasized that complete penetration could only be achieved with embryos of e9.5 to e10.5. In older embryos the detection of mRNAs was limited to the surface of the embryos. Fig. 3E roughly indicates the limit of penetration of the probes and antibodies. Sensitivity of the whole-mount in situ hybridization was comparable to in situs on sectioned material, since we were able to visualize every previously published source of SlF and c-kit mRNA in e9.5 to e10.5 embryos. However, compared to hybridization of tissue sections, the temporal and spatial resolution of the whole-mount in situ hybridizations is superior.

For immunohistochemistry, whole-mount in situ hybridized embryos were equilibrated in 20% sucrose and embedded in Tissue Tec, frozen and sectioned at 16 μm. Sections were dried on gelatin/alum-subbed slides and blocked with 0.5% BSA in PBT, incubated for 45 minutes with anti-fibronectin or anti-laminin rabbit antisera at 1/50 dilution in 0.5% BSA in PBT. After washing, secondary rhodamine-labeled goat anti-rabbit was added for 45 minutes diluted 1/100 in 0.5% BSA in PBT. Sections were washed and embedded in glycerol containing 1% n-propylgallate.

## RESULTS

### Cells expressing c-kit and TRP-2 mRNA (melanocyte precursors) in the migration staging area disperse on the dorsolateral pathway in a rostral-caudal sequence

As in previous reports (Keshet et al., 1991; Motro et al., 1991; Orr-Urtreger et al., 1990), cells expressing c-kit mRNA were observed in the head and trunk of e9.5 embryos (not shown). Although whole-mount in situ hybridization revealed c-kit mRNA in cells at various locations of e9.5 embryos, their neural crest origin could not be established. No hybridization signal was revealed by using the TRP-2 riboprobe (not shown), so melanocyte precursors could not be unequivocally identified.

By e10.5, cells located in sites usually occupied by migrating cranial crest cells can be seen to express the TRP-2 mRNA. These cells were detected between the forebrain-midbrain junction and the eye (Fig. 1B), at the level of the midbrain-hindbrain junction, and posterior to the otic vesicle. Cells expressing c-kit mRNA were also detected in these locations (Fig. 1A). Based on the time of appearance and their locations (compare with Steel et al., 1992), cells expressing both mRNAs seem likely to be the earliest crest-derived melanocyte precursors. It should be emphasized, however, that at this stage, c-kit mRNA-expressing cells were also detected in the olfactory pit, and the clefts of branchial arches I-IV, where TRP-2 mRNA expression was not detected (Fig. 1A,B). At this stage, only a few cells expressing TRP-2 or c-kit mRNA were detected at more posterior axial levels between the otic vesicle and the most rostral somites (Fig. 1A,B).

At e11, localization of TRP-2 and c-kit mRNA-expressing cells in the head is dramatically different. These cells were present in the head mesenchyme particularly in the region between the eye, forebrain and nose, and at the posterior regions of the branchial and hyoid arch. In addition, many TRP-2 as well as c-kit mRNA-expressing cells are localized in a stripe originating at the mid-to-hindbrain junction and extending towards the eye (Fig. 1E,F; arrowheads). In contrast, no TRP-2 mRNA-expressing cells could be detected in facial structures. Within the trunk, cells expressing TRP-2 mRNA were observed from the first somites to the level of the hind limb buds (Fig. 1D) in the same locations as cells expressing c-kit mRNA (Fig. 1C). These cells were variously localized in the migration staging area (MSA) just lateral to the neural tube at posterior axial levels, or further lateral over the somites at more anterior levels (Fig. 1C,D). Groups of TRP-2 or c-kit mRNA-expressing cells were present in a segmented pattern along the axis from very rostral to mid trunk levels. In addition, c-kit mRNA-positive cells were detected in the lateral mesenchyme, the dorsal neural tube (arrow in Fig. 1E), limb buds, and the posterior gut where no TRP-2 mRNA-expressing cells could be detected (Fig. 1D).

By e11.5, as previously reported (Steel et al., 1992), TRP-2 mRNA-expressing cells were detected at locations in the head mesenchyme anterior and posterior to the eye, over the hindbrain, around the otic vesicle and at the posterior aspect of the hyoid arch (Fig. 2B). In the trunk, all cells expressing TRP-2 mRNA were found distributed over the entire somite surface, but no cells were detected in the lateral mesenchyme and in the limb buds (Fig. 2A). In contrast, individual c-kit mRNA-expressing cells were found dispersed over the somite surface, but also more lateral within the lateral mesenchyme (Fig. 2C). This cell population never expressed TRP-2 mRNA. We do not yet know if these cells are crest-derived or represent a mesodermally derived population, which will require more specific probes to distinguish. Expression of c-kit mRNA in mesenchymal cells was similar to that seen at earlier stages (Fig. 1C). More caudally, at the base of the tail, cells expressing TRP-2 mRNA were localized in the MSA lateral to the neural tube, and just one or two somites more rostral cells were found over the somite lateral to the MSA (Fig. 2D). In progressively older (more rostral) somites, incrementally more cells were localized laterally, and fewer TRP-2 mRNA-expressing cells remained near the neural tube (Fig. 2E). In embryos of this age, TRP-2 mRNA-expressing cells were first observed at the base of the hind limb bud (Fig. 2E).

The temporal differences between developing segments are most distinct at the level of the hindlimb of e11.5 embryos. Accordingly, this axial region best displayed the various stages of the migration of crest cells on the lateral pathway. Therefore, embryos that had been stained as whole mounts

for TRP-2 mRNA were sectioned transversely and stained with antibodies against laminin and fibronectin to reveal the architecture of the somites (see Methods). Thus, Fig. 3A shows a bright-field view of a section at the base of the tail where two groups of TRP-2 mRNA-expressing cells can be seen (corresponding to A-B in Fig. 2D). One group of cells resides in the MSA lateral to the neural tube, and the other group was localized within the dermatome. The staining for laminin revealed the borders of the neural tube and the dermatomal epithelial tissue (Fig. 3B). A section of a different embryo at a slightly older (more rostral) axial level (corresponding to C-D in Fig. 2D) shows elongated TRP-2 mRNA-positive cells on the laminin-positive basement membrane (arrows in Fig. 3C,D). At an even more rostral level (corresponding to E-F in Fig. 2D), the epithelial dermatome has already transformed into the mesenchymal dermis, made obvious by the intense fibronectin staining (Fig. 3F). TRP-2 mRNA containing cells are evenly spread throughout the dermal mesenchyme at this axial level (see also Pavan and Tilghman, 1994, Fig. 2a).

By e12.5, cells expressing TRP-2 and c-kit mRNA were detected bordering the whisker fields and localized over the nose (Fig. 4C). The regions around the ear were also densely populated by TRP-2 mRNA-expressing cells (Fig. 4A-C). In the trunk at this stage, TRP-2 mRNA-expressing cells were present between the neural tube and the lateral midline, and some cells were seen as far ventrad as the base of the forelimb bud (Fig. 4A,B,D). No TRP-2 mRNA was detected on the ventral side of the body (Fig. 4D). Many TRP-2 mRNA-expressing cells were present on the posterior side of the hindlimb (Fig. 4C, arrow) as well as on the lateral sides of the tail.

### Steel factor mRNA is expressed in a rostrocaudal sequence in the dorsal portion of the dermatome in e10.5-12.5 mouse embryos

At e9.5, whole-mount in situ hybridization reveals SlF mRNA expression in various places in the embryo: the head mesenchyme, branchial arches, the mesenchyme posterior to the last arch, part of the gut, the tail and the kidney primordium. At this stage, no SlF mRNA could be detected within the somitic tissue of the trunk (not shown).

In the head of e10.5 embryos, SlF mRNA was detected in the mesenchyme between the telencephalon and the olfactory pit, and in the mesenchyme surrounding the otic

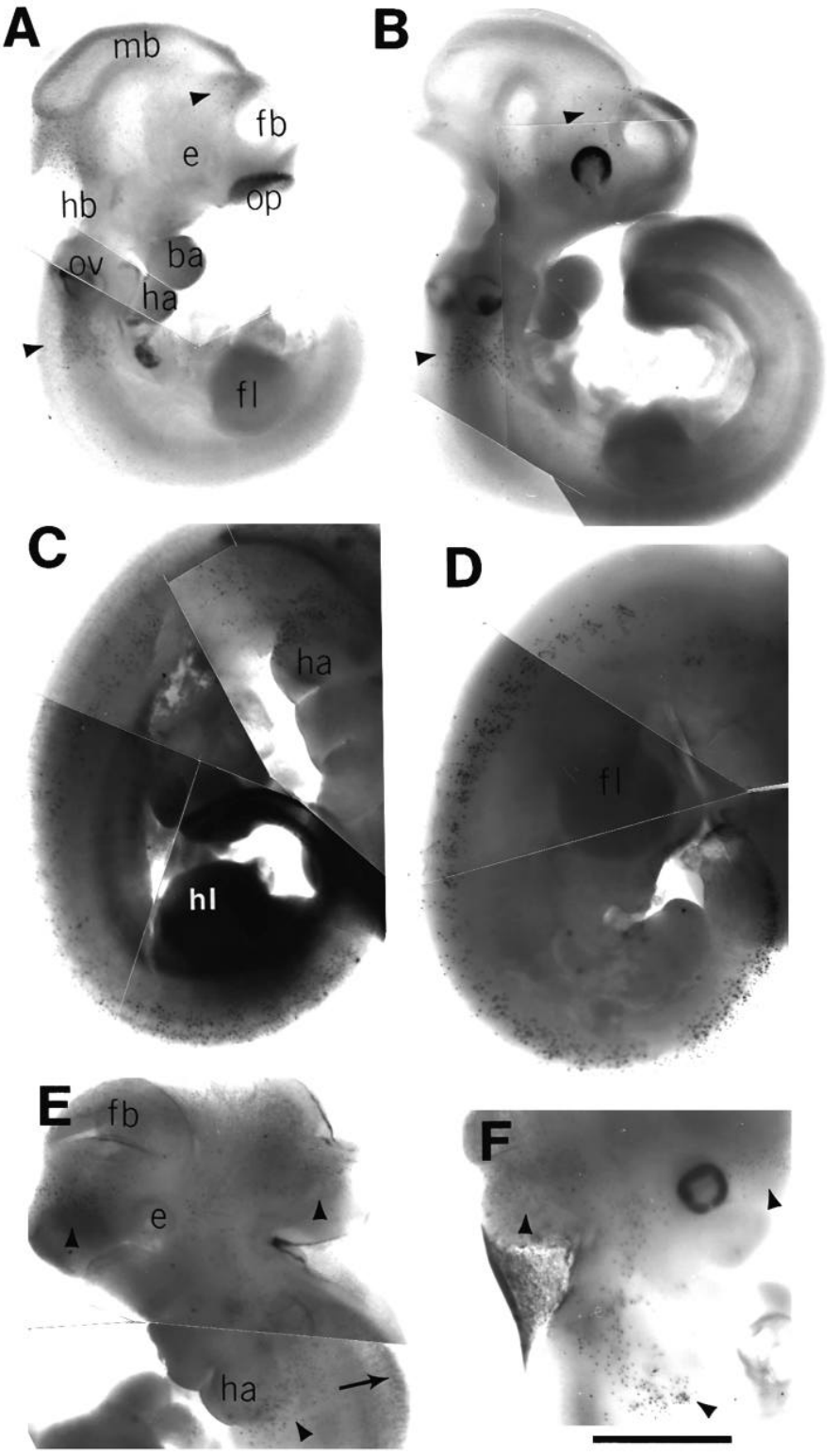


**Fig. 1.** c-kit and TRP-2 mRNA-expressing cells show a similar distribution pattern in e10.5 and e11 embryos. c-kit (left panel) and TRP-2 (right panel) antisense whole-mount in situ hybridization of e10.5 (A,B) and e11 (C,D) mouse embryos. (Note almost identical localization of punctate staining at arrowheads between c-kit and TRP-2 hybridized embryos, and the absence of forelimb and hindlimb in C and D, respectively.) The arrow in E points to c-kit mRNA expression in the spinal cord. ba, first branchial arch; e, eye; fb, forebrain; fl, forelimb; ha, hyoid arch; hb, hindbrain; hl, hindlimb; mb, midbrain; op, olfactory pit; ov, otic vesicle. Bar, 400 μm.

vesicle (see also Steel et al., 1992). SlF mRNA was also detected in the first and second branchial arches at their most posterior proximal edges (arrowheads in Fig. 5B). In the trunk of e10.5 embryos, the dermatomes express SlF mRNA in their dorsal portions. In slightly less-advanced embryos at that gestational stage, SlF mRNA was detected in dermatomes from the first somite to the midtrunk level (Fig. 5A), whereas in developmentally more advanced embryos, SlF mRNA expression was detected in dermatomes from the first somite back to somites at the hindlimb level. Transverse sections of whole-mount embryos counterstained with a polyclonal antiserum against laminin (Fig. 5K) or fibronectin (Fig. 5H) clearly localizes the SlF mRNA to the dorsal epithelial dermatome (Fig. 5G-K; see also Matsui et al., 1990). In progressively older dermatomal tissue, the location of SlF mRNA expression is shifted from the mediodorsal portion to a more dorsal location in the epithelial dermatome (Fig. 5G,I).

Embryos obtained half a gestational day later, at e11, revealed persistent SlF mRNA in the telencephalon, but expression in the cranial mesenchyme could no longer be detected. In the trunk, SlF mRNA expression is diminished in cervical somites, whereas the dorsal dermatome of all the posterior somites down to the base of the tail were strongly positive (Fig. 5C). No cells expressing SlF mRNA could be detected in the MSA (Fig. 5D).

At e11.5 SlF mRNA could no longer be detected in the head mesenchyme and the trunk somites. However the expression in the telencephalon and tail somites persisted (Fig. 5E). In addition, SlF mRNA expression was present in the posterior region of the hindlimb bud (Fig. 5F, arrow).

By e12.5, SlF mRNA expression in the telencephalon still persists, and new expression is detected in the interdigital mesenchyme of the limb buds. Expression in dorsal dermatome was detected only in the tail somites. At this stage, no hybridization signal for SlF mRNA could be detected in dermal mesenchyme associated with developing somites at more rostral axial levels (not shown).

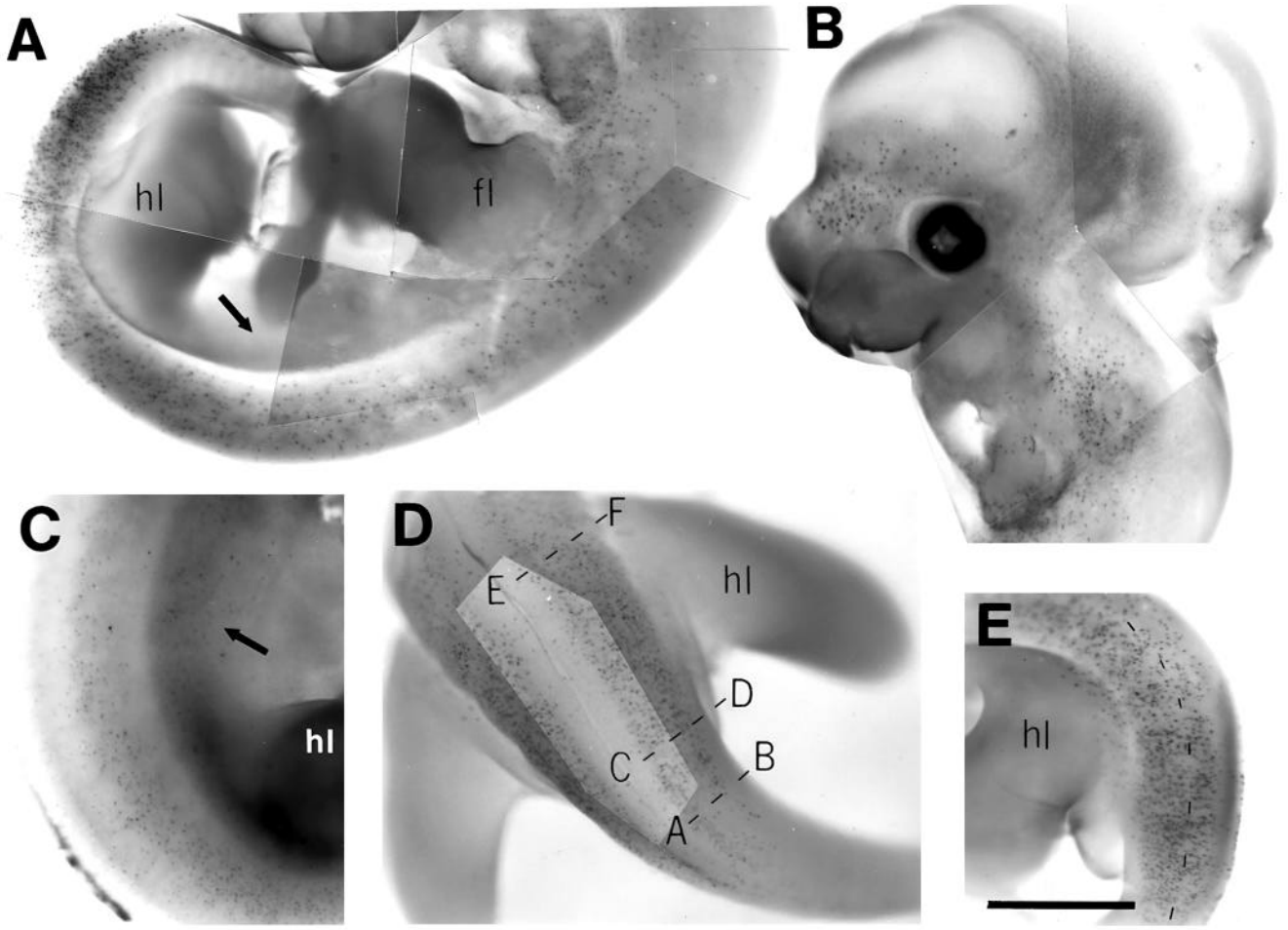


**Fig. 2.** Distribution of melanocyte precursors in e11.5 mouse embryos. TRP-2 and c-kit antisense whole-mount in situ hybridization of e11.5 embryos. (A,B) Lateral view of a TRP-2 antisense hybridization. (C) Lateral view of the mid trunk of an embryo hybridized with c-kit antisense probe. (D) Dorsal view of the tail and hindlimb buds of an embryo hybridized with TRP-2 antisense probe. The inset displays cells in the MSA that are at a higher focal level than the cells dispersing laterally on the dorsal migration pathway. (E) Lateral view of the hindlimb region of the embryo shown in A and B. The dashed line roughly indicates the lateral limit of the MSA. Note that many c-kit-positive cells can be detected in the lateral mesenchyme (arrow in C), which can not be detected with the TRP-2 probe (arrow in A). A-B, C-D and E-F approximately indicate the axial levels of transverse sections shown in Fig. 3. fl, forelimb; hl, hindlimb. Bar, 400 μm in A,B and E; 250 μm in C and 275 μm in D.

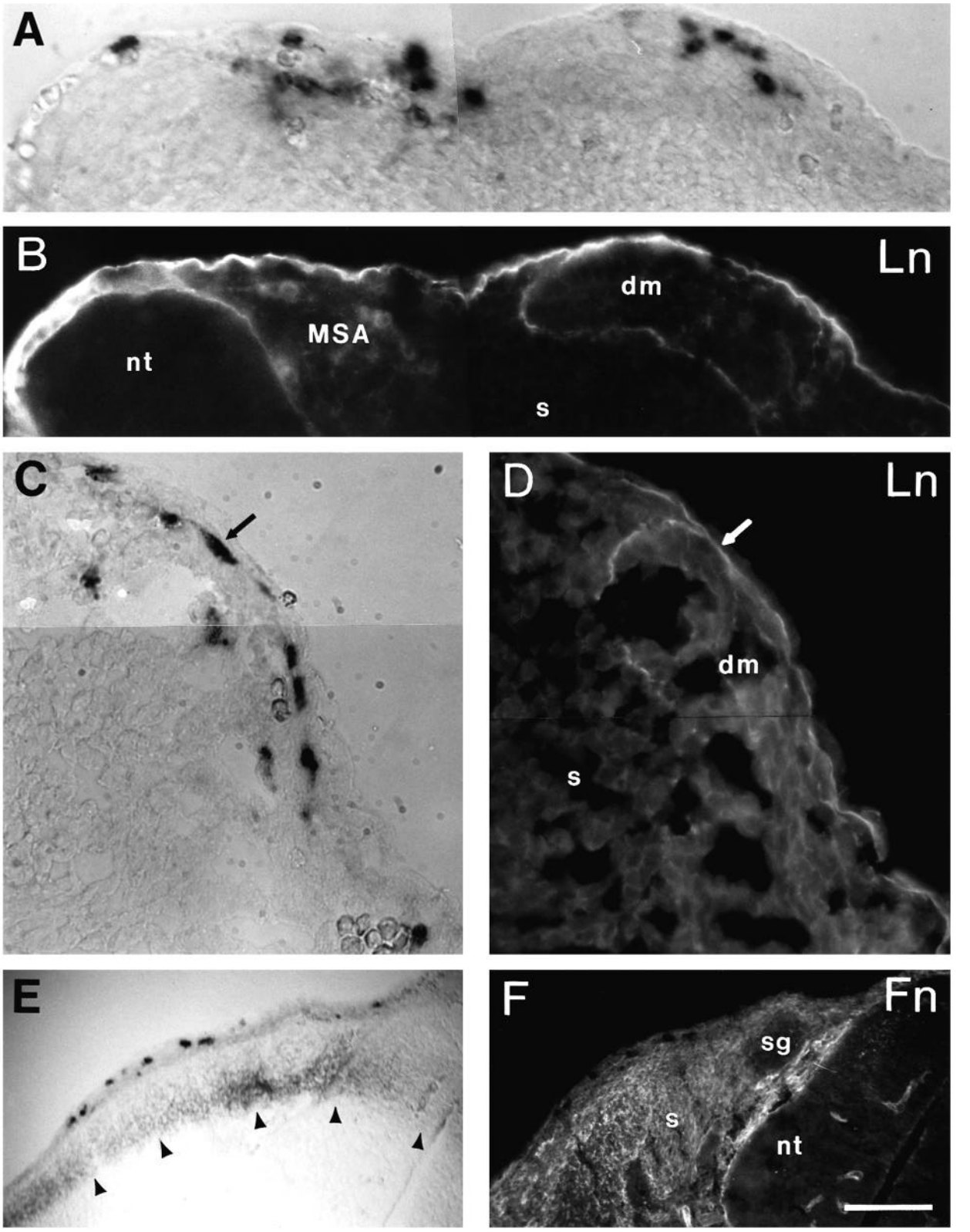


**Fig. 3.** Melanocyte precursor migration on the lateral pathway. Immunohistochemistry for laminin and fibronectin on transverse sections from an e11.5 TRP-2 antisense whole-mount in situ hybridization. Axial levels of each section are indicated in Fig. 2D. (A,C,E) Bright-field illuminations of sections corresponding to levels A-B, C-D and E-F, respectively. The sections are stained with either anti-laminin antiserum (B,D) or fibronectin antiserum (F). Note: TRP-2-positive cell elongated along a laminin-positive basement membrane (arrow in C and D). Arrowheads in E point to the penetration limit for the detection of mRNA in that particular embryo. Ln, laminin; Fn, fibronectin; nt, neural tube; dm, dermatome; s, sclerotome; MSA, migration staging area; sg, sensory ganglia. Bar, 25 μm in A-D and 100 μm in E,F.

### Migration and localization of TRP-2 mRNA-expressing cells is different in embryos homozygous for Steel alleles compared to wild-type embryos

The *Sl* null mutation and the less severe $Sl^d$ allele were used to reveal the function of SlF during melanocyte precursor migration on the lateral pathway. As above, the hindlimb level of e11.5 embryos was selected to compare melanocyte precursor migration and localization in normal and mutant embryos.

Fig. 6B shows the hindlimb level and the base of the tail of a *Sl/Sl* (null) embryo. Individual TRP-2 mRNA-expressing cells were detected in the MSA over a length of four to five segments (Fig. 6B, brackets). No cells were found more laterally on top of the dermatome. With the exception of a few cells localized to the mid-hindbrain border, no other TRP-2 mRNA-expressing cells were found in e11.5 embryos (not shown).

A $Sl^d/Sl^d$ e11.5 embryo reveals a strikingly different distribution pattern of TRP-2 mRNA-expressing cells. In addition to cells localized in the MSA, many cells were found dispersed over the somites (Fig. 6C). However, no TRP-2 mRNA-expressing cells were detected anterior to the level of the hindlimb (Fig. 6C), with the exception of some cells at the mid-hindbrain border (not shown). In contrast, in wild-type embryos, a higher density of TRP-2 mRNA-expressing cells were localized over the dermatome compared to the $Sl^d/Sl^d$ mutant embryos (Fig. 6A).

As a further test of the role of SlF function in promoting melanocyte precursor dispersal, embryos homozygous for the *W* mutation (phenotypically null for c-kit activity) were examined. Such embryos showed a pattern of TRP-2 mRNA-expressing cells in the tail region comparable to the pattern observed in *Sl/Sl* (null) embryos (Fig. 6D).

## DISCUSSION

### Melanocyte precursors arise in the migration staging area (MSA) prior to their dispersal on the lateral pathway

At e10.5, cells expressing TRP-2 and c-kit mRNA have been reported lateral to neural tube in the head (Steel et al., 1992). In the trunk c-kit-positive cells have been reported to be lateral to the neural tube between e10.5 and e11 (Manova and Bachvarova 1991). At later stages, we have observed c-kit and TRP-2 mRNA-positive cells at trunk levels posterior to the hindlimb buds (at the base of the tail). In addition to their presence in the MSA of the trunk, melanocyte precursors are known to be present initially in a few regions in the head, including the regions between brain vesicles and posterior to the otic vesicle. As has been suggested by Steel et al. (1992), it is very likely that these cells are melanocyte precursors and that they co-express both c-kit mRNA and TRP-2 mRNA. It is not yet known, but will be important to learn, what local environmental cues induce the expression of melanocyte specific genes, and when crest cells in the MSA respond to such cues.

Assuming that our marking studies do, in fact, reveal melanocyte precursors, it is of particular interest to note that

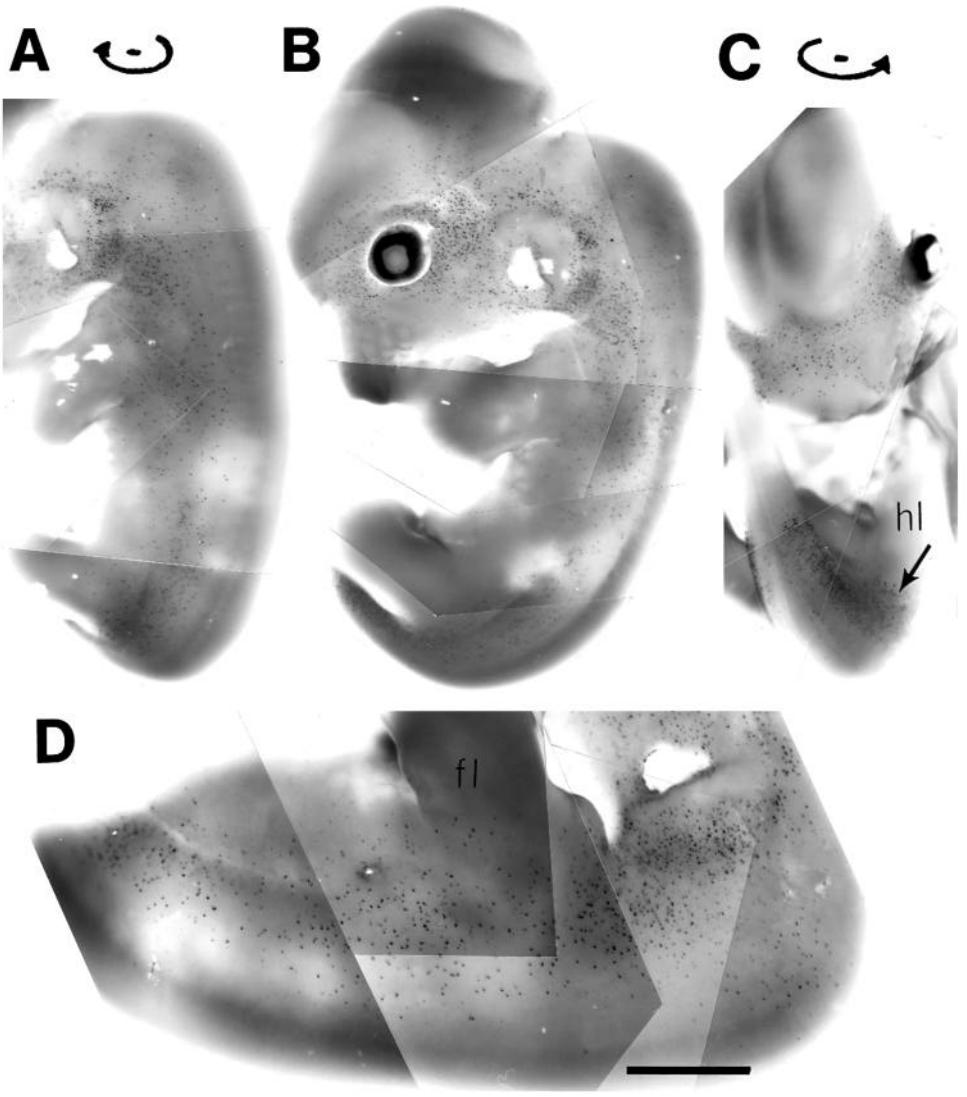


**Fig. 4.** Distribution of melanocyte precursors in e12.5 embryos. TRP-2 antisense whole-mount in situ hybridization of e12.5 mouse embryos. Alternative views are shown of one embryo in A-C. From B, the embryo is turned clockwise (A) or counter-clockwise (B) to reveal lateral and frontal views of the embryo. The lateral side of a different embryo is shown in D. Note: Arrow in C points to a population of TRP-2-positive cells entering the posterior aspect of the hindlimb. fl, forelimb; hl, hindlimb. Bar, 500 μm in A-C; 320 μm in D.

these cells appear belatedly as a subpopulation among crest-derived cells in the MSA. They seem to arise in the MSA after most of the neurogenic crest-derived cells have dispersed on the medial pathway (see Weston, 1991), but before dispersal has begun on the lateral crest migration pathway. In this regard, it is also of interest to note that Erickson and Goins (1995; personal communication) have also recently shown that older crest-derived cells that have become specified as melanocyte

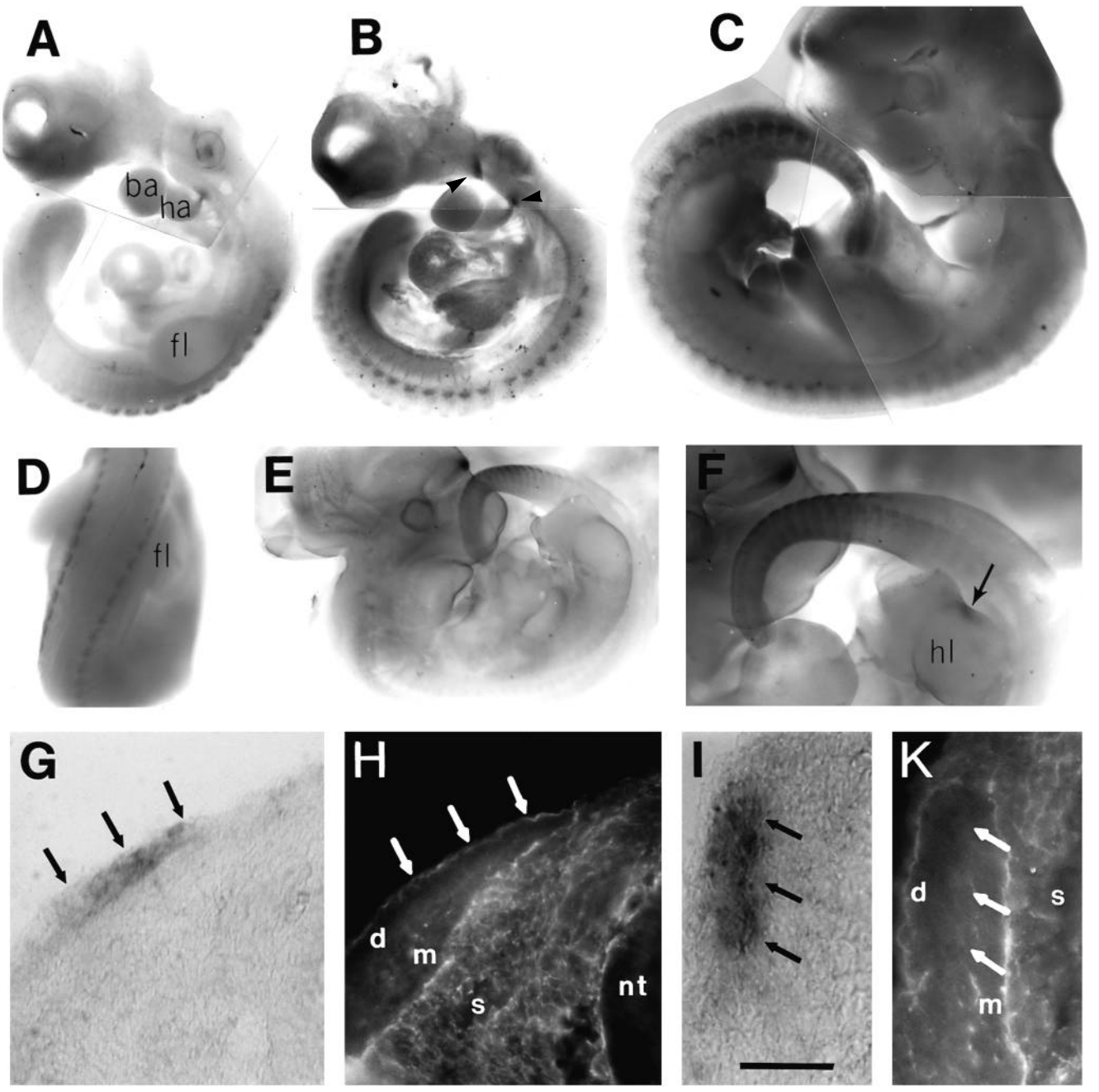


**Fig. 5.** Rostrocaudal sequence of SlF mRNA expression in the dorsal dermatome. SlF (KL-M1) antisense whole-mount in situ hybridization of e10.5, e11 and e11.5 mouse embryos and immunohistochemistry for laminin and fibronectin of e10.5 transverse sections. (A,B) Lateral view of two e10.5 embryos, A is slightly younger than B. Arrowheads point to mesenchymal SlF mRNA expression at the posterior border of the first and second branchial arches. (C) Lateral view of an e11 embryo. (D) Dorsal view of an e11 embryo. (E) Lateral view of an e11.5 embryo, a closeup of the tail region is shown in F. Note the expression of SlF mRNA in the posterior aspect of the hindlimb (arrow). Transverse sections of an e10.5 SlF whole-mount in situ hybridization from a midtrunk (G,H) and cervical (I,K) level. The dermatome shown in G,H is developmentally younger than that in I and K. Arrows mark the limits of the SlF mRNA expression. ba, first branchial arch; hyoid arch; fl, forelimb; hl, hindlimb; d, dermatome; m, myotome; s, sclerotome; nt, neural tube. Bar, 300 μm in A-C, E and F, 470 μm in D and 25 μm in G-K.

precursors can precociously invade the lateral migration pathway when they are grafted heterochronically into avian host embryos.

### Transient expression of Steel Factor mRNA by dermatomal epithelial cells precedes dispersal of melanocyte precursors on the lateral pathway

Whole-mount in situ hybridization with a probe for SlF mRNA has confirmed earlier reports of its presence in the dorsal dermatome (Matsui et al., 1990). In addition, however, this method has revealed the precise expression pattern relative to the pattern of dispersal of putative melanocyte precursors. In particular, our results demonstrate, first, that SlF mRNA expression is transiently localized to the dorsal epithelial dermatome and, second, that this expression precedes the onset of melanocyte precursor dispersal on the migration path towards the dermatome. Finally, our results indicate that SlF mRNA is down regulated in the epithelial dermatome as it de-epithelializes to produce dermal mesenchyme. It is not known how long SlF protein persists in the dermal mesenchyme, or when SlF mRNA is re-expressed by these cells (Keshet et al., 1991; Motro et al., 1991; Orr-Urtreger et al., 1990). In utero injection of anti-c-kit antibodies (Nishikawa et al., 1991) has revealed a SlF-dependent period at around e14.5, corresponding to the time (e13-14) when melanocyte precursors localized in the dermal mesenchyme are known to enter the epidermis (Mayer, 1973). Since melanocyte precursors transiently depend on SlF for survival (see also Morrison-Graham and Weston, 1993), SlF protein must be retained and made accessible for the migrating melanocyte precursors in the newly formed dermis. No data are yet available on the presence and location of SlF protein after the transformation of the dermatome into dermal mesenchyme is completed.

### Melanocyte precursors in the MSA initially disperse toward the site where SlF mRNA is transiently produced

In the head, at e11 c-kit/TRP-2 mRNA-positive cells localize to regions where SlF mRNA was detected at e10.5 (Steel et al., 1992). Likewise, melanocyte precursors disperse from the MSA

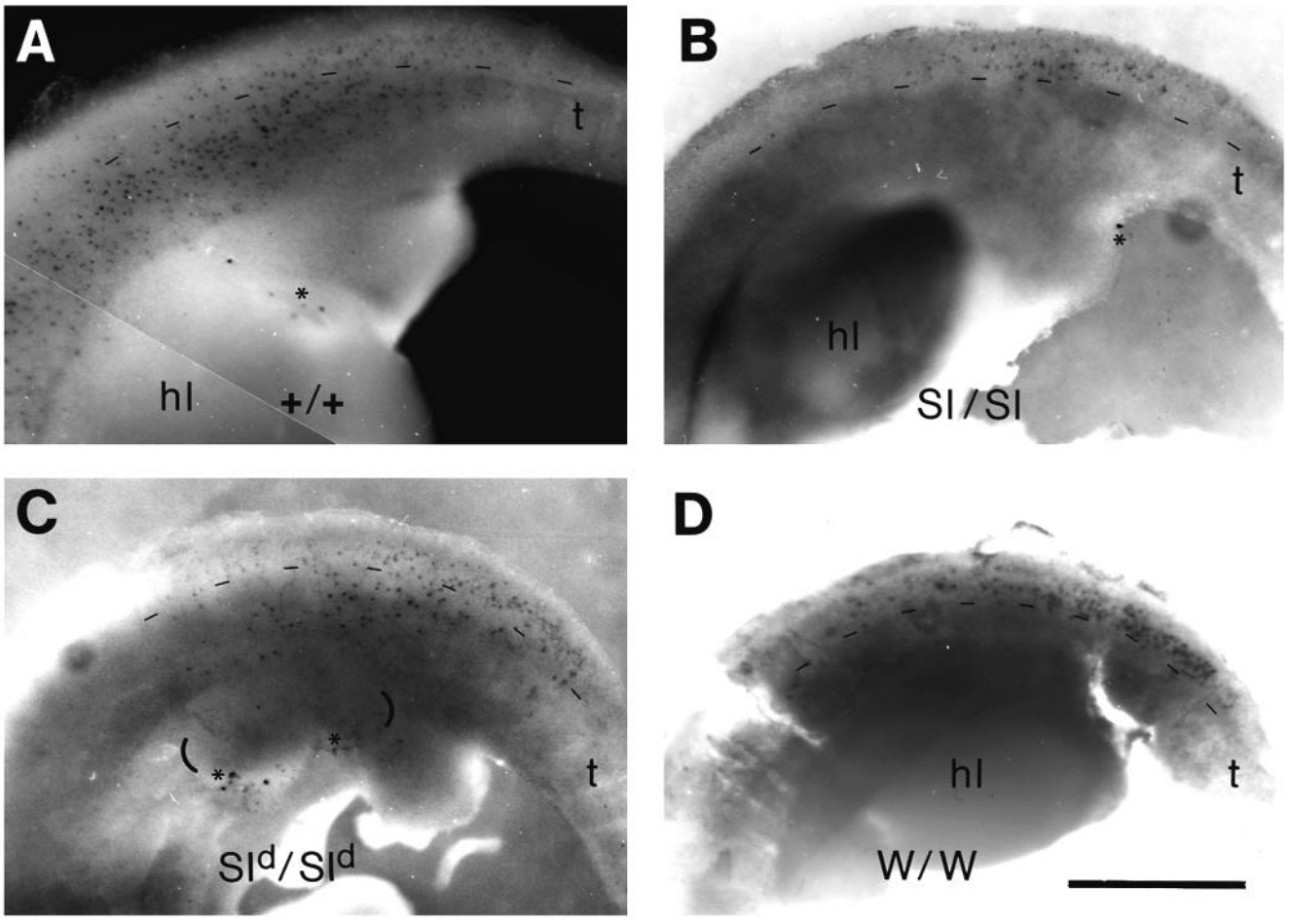


**Fig. 6.** Melanocyte precursors initially appear but behave differently in *Steel* mutant embryos. TRP-2 antisense whole-mount in situ hybridization of e11.5 mouse mutant embryos. The tail and hindlimb bud region is shown of embryos being wild type (A, +/+), homozygous for SlF null allele (B, *Sl*/*Sl*), homozygous for *Sl dickie* (C, $Sl^d/Sl^d$) or homozygous for c-kit functional null allele (D, *W/W*). The litter that contained embryo D was developmentally slightly younger than other 'e11.5' litters so that cells were seen over a wider area along the A-P axis compared to the developmentally older embryo seen in B. In addition, this embryo was stained longer than the other embryos, which affected the appearance of the stained cells. The dashed lines roughly indicate the lateral limits of the MSA. In C, the location of the limb bud, which was removed for genotyping (see Methods), is indicated with parentheses; dirt particles are marked with asterisk. hl, hindlimb; t, tail. Bar, 200 μm.

to sites where SlF mRNA had been transiently expressed about 6-12 hours previously, suggesting an influence of SlF protein on the migration and localization of melanocyte precursors. Interestingly, melanocyte precursors migrating on the lateral pathway seem to follow existing basement membranes, as do the medially migrating crest cells (Tosney et al., 1994). Two extreme models could explain the observed migration pattern. First, TRP-2/c-kit mRNA-expressing cells could migrate on both the medial and lateral pathways and survive only at locations expressing SlF. This model would imply a passive role of SlF on initial cell migration stressing only the survival effect of SlF on dependent cell populations. Alternatively, cells that express functional c-kit receptors, as implied by c-kit mRNA expression, could be selectively attracted onto the lateral pathway by SlF that is locally produced by dermatomal epithelium and diffuses from its site of expression. This notion is supported by the reports that c-kit-expressing carcinoma cells as well as c-kit transfected endothelial cells show chemotaxis towards SlF in vitro (Blume-Jensen et al., 1991; Sekido et al., 1993), and is consistent with the belated appearance of cells in the MSA that express c-kit and the corresponding delay in onset of migration on the lateral pathway. Although the initial onset of dispersal of melanocyte precursors on the lateral pathway is consistent with a chemotactic response to a source of SlF in the dermatome, the subsequent dispersal of melanocyte precursors that occurs after e11.5 in the dermal mesenchyme of the trunk, limb buds or ventral body wall, cannot be explained by a graded or localized source of SlF.

### Melanocyte precursors fail to disperse or survive in Steel null mutant embryos

If SlF were required for initial dispersal of melanocyte precursors, then these cells would be predicted to remain in the MSA in mutants that do not produce this molecule. This prediction has been verified by our observations of the behavior of TRP-2 mRNA-expressing cells in Steel null embryos. Such cells appear in the MSA in a timely way, but never disperse, and ultimately disappear. The fate of these melanocyte precursors is not known. Alternatively, their apparent failure to disperse may be the result of failing to survive in the MSA long enough to do so. We know that melanocyte precursors in vitro require transient trophic support from SlF for about 5 days (Morrison-Graham and Weston, 1993). Since the time interval during which melanocyte precursors are generated in the MSA is not known, however, it is difficult to estimate how long individual TRP-2/c-kit mRNA-expressing cells can survive in the MSA in the absence of SlF. If this period were brief, however, SlF-dependent cells would probably not survive long enough to leave the MSA. In this regard, mast cells, which are also dependent on c-kit/SlF activity, begin to degenerate in vitro within 5 hours after SlF is removed from their culture medium (Iemura et al., 1994; Caceres-Cortes et al., 1994). Survival of individual melanocyte precursors in the MSA of SlF null mutants might be even shorter because these cells would never have received an SlF stimulus.

The conclusion that crest-derived melanocyte precursors require a timely SlF stimulus in the MSA is supported by our observations that TRP-2 mRNA-expressing melanocyte precursors are initially present in the MSA, but are never found on the lateral pathway of embryos that are homozygous for the *W* mutation. Thus, cells that lack functional c-kit receptors are unable to detect the presence of SlF, and therefore either fail to survive in the MSA or are unable to depart on the lateral pathway in response to a directional SlF signal.

### Soluble SlF is sufficient to permit initial dispersal of melanocyte precursors from the MSA onto the lateral pathway, but not for eventual survival and/or differentiation

The *Steel dickie* ($Sl^d$) mutation results in a truncated but biologically active form of SlF that lacks a transmembrane domain (Brannan et al., 1991). The lack of a transmembrane anchor results in the secretion of SlF by cells from $Sl^d$ homozygotes (Flanagan et al., 1991). Since $Sl^d$ homozygotes exhibit an intermediate phenotype compared to *Sl* null mutants, the membrane-bound SlF appears to be required for normal development of these cells.

Paradoxically, neural crest cell cultures are able to give rise to melanocytes in vitro when cultured in the presence of exogenous soluble SlF (Morrison-Graham and Weston, 1993), or on detergent-extracted (cell-free) extracellular matrix (ECM) deposited by wild-type embryonic skin fibroblast in vitro (Morrison-Graham et al., 1990). ECM deposited by such cells seems to contain enough SlF to satisfy the SlF-dependent melanocyte precursors in vitro. In contrast, detergent-extracted ECM deposited by cultured fibroblasts from $Sl^d$ homozygotes fail to support melanogenesis in vitro (Morrison-Graham et al., 1990), suggesting that the truncated SlF is not incorporated or retained in ECM secreted by these cells to permit survival and/or differentiation of melanocyte precursors.

Heterochronic grafting experiments (Erickson and Goins, 1995; personal communication) indicate that melanocyte precursors arise late and invade the dorsolateral migration pathway in response to some localized cue(s) in the avian embryo. It seems likely that the soluble form of SlF may be at least one such cue. Thus, in the present report, it is of particular interest that crest-derived melanocyte precursors do, in fact, leave the MSA on the lateral pathway in $Sl^d$ homozygotes, suggesting that the truncated (soluble) SlF produced by the dorsal dermatome is sufficient for crest cells to initiate dispersal on the lateral pathway. However, since these dispersing melanocyte precursors fail to survive in the dermal mesenchyme, the truncated SlF appears not to provide an appropriate survival stimulus in the dermatomal ECM.

Taken together, the behavior and fate of melanocyte precursors in the null mutant compared to that in normal embryos or the $Sl^d$ homozygotes suggests that cell-bound and soluble SlF have distinct functions. Although it is not known how much SlF is normally released by dermatomal cells and is present in interstitial crest migration spaces, it seems likely that soluble SlF might be required to promote dispersal of c-kit mRNA-expressing melanocyte precursors, or to attract them to its local source. Likewise, the behavior and fate of melanocyte precursors in $Sl^d$ embryos suggests that an 'immobilized' form of SlF is required for survival of the responsive cell type. Three published reports support our inference that soluble and cell-bound SlF play distinct roles in cell dispersal and survival, respectively. First, in the head of $Sl^d$ embryos, TRP-2 mRNA-expressing cells appear initially and disperse, but then disappear (Steel et al., 1992). Second, germ cells, which are known to require SlF and c-kit for survival can be found in small numbers at the genital ridges in $Sl/Sl^d$ embryos

(McCoshen and McCallion, 1975), whereas in *Steel* null mutant embryos, germ cells do not proliferate and are retarded in their migration to the genital ridges (Mintz and Russell, 1957). Finally, on a fibronectin substratum in vitro, motility of mast cells, which are strictly dependent on c-kit for survival, is stimulated by an SlF dose which is 100-fold less than that required for survival (Kinashi and Springer, 1994; Dastych and Metcalf, 1994). Therefore different concentration of SlF in the cell environment may induce motogenic versus mitogenic responses (Blume-Jensen et al., 1993).

We are grateful to Drs Yoshiko Takahashi and Carol Erickson, who worked in our laboratory on preliminary experiments leading to this paper, and to Monique Wehrle-Haller, Drs Erickson, K. Morrison-Graham and Sherry Rogers, for their critical comments on the manuscript. We also thank Drs John Flanagan, Ian Jackson, Robert Arceci for generously providing cDNA plasmids and Dr Peter Lonai for sharing primer sequences. Special thanks to Rick Gosswiller, for his careful animal husbandry and Jerry Gleason for photographic assistance. Our work has been supported by grant DE-04316 from the USPHS. B. W-H is supported by an EMBO Postdoctoral Fellowship (169-1993). Dr Erickson's work in our laboratory was supported by grant DE-05620 from the USPHS.

## REFERENCES

**Anderson, D., Lyman, S., Baird, A., Wignall, J., Eisenman, J., Rauch, C., March, C. J., Boswell, H., Gimpel, S., Cosman, D. and Williams, D.** (1990). Molecular cloning of mast cell growth factor a hematopoietin that is active in both membrane bound and soluble forms. *Cell* **63**, 235-243.

**Blume-Jensen, P., Claesson-Welsh, L., Siegbahn, A., Zsebo, K., Westermark, B. and Heldin, C.** (1991). Activation of the human c-*kit* product by ligand-induced dimerization mediates circular actin reorganization and chemotaxis. *EMBO J.* **10**, 4121-4128.

**Blume-Jensen, P., Siegbahn, A., Stabel, S., Heldin, C. and Roennstrand, L.** (1993). Increased kit/SCF receptor induced mitogenicity but abolished cell motility after inhibition of protein kinase C. *EMBO J.* **12**, 4199-4209.

**Brannan, C., Lyman, S., Williams, D., Eisenman, J., Anderson, D., Cosman, D., Bedell, M., Jenkins, N. and Copeland, N. G.** (1991). *Steel-dickie* mutation encodes a c-kit ligand lacking transmembrane and cytoplasmic domains. *Proc. Natl. Acad. Sci. USA* **88**, 4671-4674.

**Caceres-Cortes, J., Rajotte, D., Dumouchel, J., Haddad, P. and Hoang, T.** (1994). Product of the *Steel* locus suppresses apoptosis in hematopoietic cells. *J. Biol. Chem.* **269**, 12084-12091.

**Copeland, N., Gilbert, D., Cho, B., Donovan, P., Jenkins, N., Cosman, D., Anderson, D., Lyman, S. and Williams, D.** (1990). Mast cell growth factor maps near the *Steel* locus on mouse chromosome 10 and is deleted in a number of *Steel* alleles. *Cell* **63**, 175-183.

**Dastych, J. and Metcalf, D.** (1994). Stem cell factor induces mast cell adhesion to fibronectin. *J. Immunol.* **152**, 213-219.

**Derby, M.** (1978). Analysis of glysosaminoglycans within the extracellular environments encountered by migrating neural crest cells. *Dev. Biol.* **66**, 321-336.

**Duttlinger, R., Manova, K., Chu, T., Gyssler, C., Zelenetz, A., Bachvarova, R. F. and Besmer, P.** (1993). *W-sash* affects positive and negative elements controlling *c-kit* expression: ectopic *c-kit* expression at sites of kit-ligand expression affects melanogenesis. *Development* **118**, 705-717.

**Erickson, C. and Loring, J.** (1987). Neural crest cell migratory pathways in the trunk of the chick embryo. *Dev. Biol.* **121**, 220-236.

**Erickson, C. and Goins, T. M.** (1995). Neural crest cells can migrate in the dorsolateral path only if they are specified as pigment cells. *Development* (in press).

**Erickson, C., Duong, T. and Tosney, K.** (1992). Descriptive and experimental analysis of dispersion of neural crest cells along the dorsolateral path and their entry into ectoderm in the chick embryo. *Dev. Biol.* **151**, 251-271.

**Flanagan, J. and Leder P.** (1990). The *kit* ligand: a cell surface molecule altered in *Steel* mutant fibroblasts. *Cell* **63**, 185-194.

**Flanagan, J., Chan, D. and Leder P.** (1991). Transmembrane form of the kit ligand growth factor is determined by alternative splicing and is missing in the $Sl^d$ mutant. *Cell* **64**, 1025-1035.

**Geissler, E., Ryan, M. and Housman, D. E.** (1988). The dominant-white spotting (W) locus of the mouse encodes the c-kit proto-oncogene. *Cell* **55**, 185-192.

**Hayashi, S., Kunisade, T., Ogawa, M., Yamaguchi, K. and Nishikawa, S.** (1991). Exon skipping by mutation of an authentic splice site of c-*kit* gene in *W/W* mouse. *Nuc. Acids. Res.* **19**, 1267-1271.

**Huang, E., Nocka, K., Beier, D. R., Chu, T., Buck, J., Lahm, H., Wellner, D., Leder, P. and Besmer, P.** (1990). The hematopoietic growth factor KL is encoded by the *Sl* locus and is the ligand of the *c-kit* receptor, the gene product of the *W* locus. *Cell* **63**, 225-233.

**Huang, E., Nocka, K., Buck, J. and Besmer, P.** (1992). Differential expression and processing of two cell associated forms of the kit-ligand: Kl-1 and Kl-2. *Mol. Biol. Cell* **3**, 349-362.

**Iemura, A., Tsai, M., Ando, A., Wershil, B. and Galli, S.** (1994). The c-*kit* ligand, stem cell factor, promotes mast cell survival by suppressing apoptosis. *Am. J. Pathol.* **144**, 321-328.

**Keshet, E., Lyman, S., Williams, D., Anderson, D., Jenkins, N., Copeland, N. and Parada, L.** (1991). Embryonic RNA expression patterns of the c-*kit* receptor and its cognate ligand suggest multiple functional roles in mouse development. *EMBO J.* **10**, 2425-2435.

**Kinashi, T. and Springer, T.** (1994). Steel factor and *c-kit* regulate cell-matrix adhesion. *Blood* **83**, 1033-1038.

**Manova, K. and Bachvarova, R.** (1991). Expression of c-*kit* encoded at the *W* locus of mice in developing embryonic germ cells and presumptive melanoblasts. *Dev. Biol.* **146**, 312-324.

**Matsui, Y., Zsebo, K. and Hogan, B.** (1990). Embryonic expression of a hematopoietic growth factor encoded by the *Sl* locus and the ligand for c-kit. *Nature* **347**, 667-669.

**Mayer, T. C.** (1973). The migratory pathway of neural crest cells into the skin of mouse embryos. *Dev. Biol.* **34**, 39-46.

**McCoshen, J. and McCallion, J.** (1975). A study of the primordial germ cells during their migratory phase in *Steel* mutant mice. *Experientia* **31**, 589-590.

**Mintz, B. and Russell, E. S.** (1957). Gene-induced embryological modifications of primordial germ cells in the mouse. *J. Exp. Zool.* **134**, 207-237.

**Morrison-Graham, K., West-Johnsrud, L. and Weston, J.** (1990). Extracellular matrix from normal but *Steel* mutant mice enhances melanogenesis in cultured mouse neural crest cells. *Dev. Biol.* **139**, 299-307.

**Morrison-Graham, K. and Takahashi, Y.** (1993). Steel factor and c-kit receptor: from mutants to a growth factor system. *BioEssays* **15**, 77-83.

**Morrison-Graham, K. and Weston J.** (1993). Transient Steel factor dependence by neural crest-derived melanocyte precursors. *Dev. Biol.* **159**, 346-352.

**Motro, B., Van der Kooy, D., Rossant, J., Reith, A. and Bernstein, A.** (1991). Contiguous patterns of c-*kit* and *Steel* expression: analysis of mutations at the *W* and *Sl* loci. *Development* **113**, 1207-1221.

**Nishikawa, S., Kusakabe, M., Yoshinaga, K., Ogawa, M., Hayashi, S., Kunisade, T., Era, T., Sakakura, T. and Nishikawa, S.** (1991). *In utero* manipulation of coat color formation by a monoclonal anti-*c-kit* antibody: two distinct waves of *c-kit* dependency during melanocyte development. *EMBO J.* **10**, 2111-2118.

**Nocka, K., Buck, J., Levi, E. and Besmer, P.** (1990a). Candidate ligand for the c-*kit* transmembrane kinase receptor: KL, a fibroblast derived growth factor stimulates mast cells and erythroid progenitors. *EMBO J.* **9**, 3287-3294.

**Nocka, K., Tan, J., Chiu, E., Chu, T., Ray, P., Traktman, P. and Besmer, P.** (1990b). Molecular bases of dominant negative and loss of function mutations at the murine c-kit/white spotting locus: $W^{37}$, $W^{v}$, $W^{41}$, and *W*. *EMBO J.* **9**, 1805-1813.

**Orr-Urtreger, A., Avivi, A., Zimmer, Y., Givol, D., Yarden, Y. and Lonai, P.** (1990). Developmental expression of c-kit, a proto-oncogene encoded by the *W* locus. *Development* **109**, 911-923.

**Orr-Urtreger, A., Bedford, M., Do, M.-S., Eisenbach, L. and Lonai, P.** (1992). Developmental expression of the a receptor for platelet-derived growth factor, which is deleted in the embryonic lethal *Patch* mutation. *Development* **115**, 289-303.

**Pavan, W. and Tilghman, S.** (1994). Piebald lethal ($s^l$) acts early to disrupt the development of neural crest-derived melanocytes. *Proc. Nat. Acad. Sci. USA* **91**, 7159-7163.

**Rawles, M. E.** (1947). Origin of pigment cells from the neural crest in the mouse embryo. *Physiol. Zool.* **20**, 248-265.

**Sekido, Y., Takahashi, T., Ueda, R., Takahashi, M., Suzuki, H., Nishida, K., Tsukamoto, T., Hida, T., Shimokata, K., Zsebo, K. M. and**

**Takahashi, T.** (1993). Recombinant human stem cell factor mediates chemotaxis of small-cell lung cancer cell lines aberrantly expressing the c-*kit* proto-oncogene. *Cancer Res.* **53**, 1709-1714.

**Steel, K., Davidson, D. and Jackson, I.** (1992). TRP-2/DT, a new early melanoblast marker, shows that Steel growth factor (c-kit ligand) is a survival factor. *Development* **115**, 111-1119.

**Tosney, K., Dehnbostel, D. and Erickson, C. A.** (1994). Neural crest cells prefer the myotome's basal lamina over the sclerotome as a substratum. *Dev. Biol.* **163**, 389-406.

**Wang, C., Kelly, J., Bowen-Pope, D. and Stiles, C.** (1990). Retinoic acid promotes transcription of the platelet-derived growth factor alpha receptor gene. *Mol. Cell Biol* **10**, 6781-6784.

**Weston J. A.** (1991). Sequential segregation and fate of developmentally restricted intermediate cell populations in the neural crest lineage. *Cur. Topics Dev. Biol.* **25**, 133-153.

**Williams, D., Eisenman, J., Baird, A., Rauch, C., Van Ness, K., March, C., Park, L. S., Martin, U., Mochizuki, D., Boswell, H., Burgess, G., Cosman, D. and Lyman, S. D.** (1990). Identification of a ligand for the c-*kit* proto-oncogene. *Cell* **63**, 167-174.

**Williams, D., De Vries, P., Namen, A., Widmer, M. and Lyman, S.** (1992). The *Steel* factor. *Dev. Biol.* **151**, 368-376.

**Yamaguchi, T., Conlon, R. and Rossant, J.** (1992). Expression of the fibroblast growth factor receptor FGFR-1/flg during gastrulation and segmentation in the mouse embryo. *Dev. Biol.* **152**, 75-78.

**Yoshida, H., Nishikawa, S., Okamura, H., Sakakura, T. and Kusakabe, M.** (1993). The role of c-*kit* proto-oncogene during melanocyte development in mouse. *in vivo* approach by the *in utero* microinjection of anti-c-kit antibody. *Dev. Growth Differ.* **35**, 209-220.

(Accepted 28 October 1994)